Transportation Research Part D 67 (2019) 263–274

Contents lists available at ScienceDirect

Transportation Research Part D

journal homepage: www.elsevier.com/locate/trd

Life cycle assessment of permanent magnet electric traction motors

Anders Nordelöf[a,*], Emma Grunditz[b], Sonja Lundmark[b], Anne-Marie Tillman[a], Mikael Alatalo[b], Torbjörn Thiringer[b]

[a] Chalmers University of Technology, Division of Environmental Systems Analysis, 412 96 Gothenburg, Sweden
[b] Chalmers University of Technology, Division of Electric Power Engineering, 412 96 Gothenburg, Sweden

ARTICLE INFO

Keywords:
Life cycle assessment (LCA)
Magnet
Electric motor
Neodymium
Samarium
Ferrite

ABSTRACT

Ongoing development of electrified road vehicles entails a risk of conflict between resource issues and the reduction of greenhouse gas emissions. In this study, the environmental impact of the core design and magnet material for three electric vehicle traction motors was explored with life cycle assessment (LCA): two permanent magnet synchronous machines with neodymium-dysprosium-iron-boron or samarium-cobalt magnets, and a permanent magnet-assisted synchronous reluctance machine (PM-assisted SynRM) with strontium-ferrite magnets. These combinations of motor types and magnets, although highly relevant for vehicles, are new subjects for LCA. The study included substantial data compilation, machine design and drive-cycle calculations. All motors handle equal take-off, top speed, and driving conditions. The production (except of magnets) and use phases are modeled for two countries – Sweden and the USA – to exemplify the effects of different electricity supply. Impacts on climate change and human toxicity were found to be most important. Complete manufacturing range within 1.7–2.0 g CO_2-eq./km for all options. The PM-assisted SynRM has the highest efficiency and lowest emissions of CO_2. Copper production is significant for toxicity impacts and effects on human health, with problematic emissions from mining. Resource depletion results are divergent depending on evaluation method, but a sensitivity analysis proved other results to be robust. Key motor design targets are identified: high energy efficiency, slender housings, compact end-windings, segmented laminates to reduce production scrap, and easy disassembly.

1. Introduction

1.1. Background

Worldwide, the need to radically reduce emissions of greenhouse gases from road traffic motivates the development of electrified vehicles. Meanwhile, resource constraints and supply risks gain increasing focus, e.g. in the European initiative for a circular economy and through the classification of specific metals concerning criticality (European Commission, 2015, 2018; Graedel et al., 2015). However, there is a risk of conflict between resource efficiency and the reduction of greenhouse gas emissions. For example, as a consequence of vehicle electrification, more advanced materials and processing is required to produce the powertrain components

* Corresponding author.
E-mail addresses: anders.nordelof@chalmers.se (A. Nordelöf), emma.grunditz@chalmers.se (E. Grunditz), sonja.lundmark@chalmers.se (S. Lundmark), anne-marie.tillman@chalmers.se (A.-M. Tillman), alatalo@chalmers.se (M. Alatalo), torbjorn.thiringer@chalmers.se (T. Thiringer).

https://doi.org/10.1016/j.trd.2018.11.004

Available online 11 December 2018
1361-9209/ © 2018 Elsevier Ltd. All rights reserved.

(Nordelöf et al., 2014). In addition, there is a general increase in the use of scarce and critical materials in vehicles, driven not only by electrification, but also by the increasing use of electronics for other purposes and lightweight materials (Andersson et al., 2016).

In the case of electric traction motors, a variety of design options are available, and no single solution is optimal when the pursuit of high efficiency and compact size is set against cost and long term material supply (Ramakrishnan et al., 2016; Sizov et al., 2011). Instead, design choices become a matter of prioritizing requirements. Today, the majority of all electric vehicle models on the world market use traction motors based on the strongest available permanent magnets, made of neodymium-dysprosium-iron-boron, Nd(Dy)FeB (Chan, 2007; Grunditz and Thiringer, 2016; Miller, 2013; Nakada et al., 2014), despite high cost and the fact that appropriate recycling methods have not yet been developed on an industrial scale (Koltun and Tharumarajah, 2014; Söderman and Ingemarsdotter, 2014).

Life cycle assessment (LCA) can be used to analyze the benefits and drawbacks of different design options in terms of environmental impact, for example the balance between resource extraction versus greenhouse gas emissions. Many LCA studies have been published about electric vehicles, some of which address various complete vehicles (Hawkins et al., 2012; Nordelöf et al., 2014), while others focus on the traction batteries (Ellingsen et al., 2016; Peters et al., 2017), since these are the largest contributors to the environmental load. However, only two studies were found that focus on traction motors for electric vehicles (Hernandez et al., 2017a, 2017b). In one of their studies, Hernandez et al. (2017b) compare a permanent magnet-assisted synchronous reluctance machine (PM-assisted SynRM), equipped alternatively with neodymium-iron-boron (i.e. without dysprosium additions) or manganese-zinc ferrite magnets, and compare the impacts over the complete life cycle, concluding that the machine efficiency in the use phase is the most important factor for the results. In their other study, Hernandez et al. (2017a) focus on resource depletion for the same motor type. However, neither of these two studies takes scrap losses during production into consideration. In addition, a recent thorough investigation of the underlying manufacturing data sources, both for the neodymium-iron-boron magnet production (Sprecher et al., 2014a, 2014b) and for the motor assembly (ABB, 2002), revealed inaccuracies and a need of revision to ensure their relevance for a traction motor study (Nordelöf and Tillman, 2018). Since then, additional, comprehensive life cycle inventory (LCI) data for the design and production of a Nd(Dy)FeB permanent magnet synchronous machine (PMSM) suitable for vehicle propulsion has been published in the context of a scalable LCI model (Nordelöf et al., 2018; Nordelöf and Tillman, 2018).

1.2. Aim and content of the article

The purpose of this paper is to present an LCA study of electric vehicle traction motors with three different core designs: a PMSM with Nd(Dy)FeB magnets, a PMSM with samarium-cobalt (SmCo) magnets, and a PM-assisted SynRM with strontium-ferrite (Sr-ferrite) magnets. The work was based on the newly published scalable PMSM LCI model (Nordelöf et al., 2018; Nordelöf and Tillman, 2018), but also includes substantial additional data compilation and technical investigations, especially for the use phase of all included options and the manufacturing of the SmCo PMSM and PM-assisted SynRM alternatives, as well as for the rare-earth element (REE) production chain and economic data for allocation procedures.

Hence, the overall aim of this article is to supplement and challenge previous work by presenting a study based on extensive amounts of new data, and to expand the technical scope to include additional motor types and three new magnet materials of high relevance for automotive applications. Unlike previous studies, the scope includes the use of detailed new fabrication data for all magnet types, for electrical steel manufacture and a complete motor factory. A supplementary aim is to exemplify how the previously mentioned scalable LCI model (Nordelöf et al., 2018; Nordelöf and Tillman, 2018) can be used to conduct LCA.

After the introduction, this paper presents the following sections: the goal and scope definition of the study; the inventory analysis with a description of each motor, their manufacturing procedures and how the use phase was modeled; and lastly, a presentation and discussion of impact assessment results, a robustness assessment and a concluding discussion about the implications for design and potential recovery of materials.

A supplementary information report (hereinafter abbreviated SR) is related to this article. It presents additional details about the design alternatives, the manufacturing procedures, the use phase evaluation, and the impact assessment results. The SR also explains technical terms and present simplified electric motor theory for the PM-assisted SynRM. For further such information, please read the underlying LCI model report (Nordelöf et al., 2017). All figures and tables denoted with an S refer to the SR.

2. Methods, goal and scope

2.1. Goal definition

This study was conducted to explore the environmental impact related to the choice of core design and magnet material in electrical machines intended for propulsion of vehicles. The primary target audience consists of companies that develop and manufacture electric traction motors for automotive applications, or those who make purchase requests for such machines. The intention is to support the work of balancing different requirements, both on the component and powertrain level, by providing information about how the environmental load alters with the rotor cross section design, including the magnets, and resulting shifts in the motor core size and the efficiency. Other anticipated recipients are governmental agencies and academic researchers addressing automotive technology development or environmental assessment of vehicles.

2.2. Objects of study and functional unit

Three electric motor options were compared in the study: (1) a PMSM equipped with Nd(Dy)FeB magnets, (2) a PMSM equipped with SmCo magnets, and (3) a PM-assisted SynRM equipped with ceramic Sr-ferrite magnets. A selected number of performance parameters were kept constant between the compared alternatives: all motors can provide and handle the same take-off (i.e. equal ability to provide torque for acceleration 0–50 km/h, taking 3.2–3.3 s for all options), top speed (145 km/h), and test cycle operating points in the drive cycle selected for the use phase energy efficiency evaluation, the "worldwide harmonized light duty driving test cycle" (WLTC). However, the machines were allowed to differ in acceleration performance above the nominal base speed, and they have slightly varying peak power ratings: 100 kW for the Nd(Dy)FeB PMSM, 97 kW for the SmCo PMSM, and 95 kW for the Sr-ferrite PM-assisted SynRM.

The functional unit is one driven kilometer. Each motor fulfilling the above stated performance parameters was assumed to withstand a total driven distance of 200,000 km on the selected drive cycle (the WLTC) over its lifelength. The total driven distance assumption was based on an engineering judgement by the authors, matching common assumptions made in LCA studies of electric vehicles (Nordelöf et al., 2014).

2.3. Type of LCA and life cycle scope

The study was conducted as an attributional LCA, for two key reasons. Firstly, consequential LCA (the alternative approach) leads to system expansion which means, among other things, that each option would be credited with environmental loads of processes (outside the current system boundaries) that are avoided during relevant use of co- or by-products from the studied system. For example, in the case of magnet materials, this would require identification of and data collection for several other products where co-produced REEs have relevant use. It was neither possible nor meaningful to carry out such an extension of the scope within this study. Secondly, it was found to be valuable to make the study additive, which is a key feature of the attributional format, with collected data and calculated results thereby constituting a building block for the future.

In terms of life cycle stages, the study includes production and use of the motors, but not the end-of-life (EoL) stage, where recycling and disposal of parts can take place. The literature describing current EoL for electric traction motors indicates considerable uncertainty, and a lack of representative inventory data (Andersson et al., 2016; Binnemans et al., 2013; Brahmst, 2006; Cullbrand et al., 2015; Jin et al., 2016; Söderman and Ingemarsdotter, 2014; Tasala Gradin et al., 2013; Walton et al., 2015; Zakotnik and Tudor, 2015). Practices appear to be changing as well as diverging geographically, for example between Sweden and the USA (Brahmst, 2006; Cullbrand et al., 2015). Electrical machines are sometimes disassembled from the vehicle, but are probably often still shredded along with the vehicle (Brahmst, 2006; Cullbrand et al., 2015; Tasala Gradin et al., 2013). Steel and aluminum are primarily recycled from blended pieces of milled metal (Andersson et al., 2016; Brahmst, 2006). Copper is also recovered, but there are losses into both steel and aluminum, and the separation of copper from combined material streams involves multiple steps, including international scrap trade and a lot of manual handling (Brahmst, 2006). Accordingly, the load and degree of copper recycling back to original quality is uncertain (Brahmst, 2006; Söderman and Ingemarsdotter, 2014). Similarly, almost no large scale recycling of magnet materials occurs in any country at present (Andersson et al., 2016; Binnemans et al., 2013), although new recycling methods of rare earth magnets are being researched (Walton et al., 2015; Zakotnik and Tudor, 2015). However, future efforts towards magnet recycling will involve a number of challenges, for example large scale dismantling and collection of magnets at relevant facilities (Jin et al., 2016; Walton et al., 2015).

Given the uncertainty and variability of EoL, the scope of the study was delimited to the life cycle stages in which the target group can influence the technical system, and a more in-depth investigation of motor EoL was left for future studies. Still, some general design implications for recycling are discussed in the concluding section, in relation to the overview provided above.

By necessity in terms of scope, the variation and detail for the use phase as well as the background system was delimited to enable transparency and distinct analysis. Accordingly, the use phase of each motor is presented and compared with focus on one drive cycle, intentionally selected to be as broadly representative as possible. However, six additional drive cycles were also evaluated, in the form of a use phase robustness assessment. The data which represents the background system, i.e. the upstream material and electricity production, and the transports, is characterized by vast numbers of different possible inputs, forming the context of the study. All such data was modeled with Ecoinvent (Weidema et al., 2013; Wernet et al., 2016) version 3.3 data, representing the global or regional average supply (process inputs), or national supply (electricity).

2.4. Other system boundaries and procedural aspects

In terms of geography, it was assumed that the magnets are produced in China, with this being such a key producing country in the world. Other subparts, the motor assembly and the use phase were modeled as taking place in two alternative countries: (a) in Sweden or (b) in the USA. The idea was to compare two different yet informative scenarios for the emissions caused by electricity generation. Ecoinvent data was used for the electricity supply mix of each country, both in manufacturing and for charging. This data had been extrapolated to represent year 2016, but was based on statistics from 2012 for production volumes and trading across borders (Treyer and Bauer, 2016a, 2016b; Weidema et al., 2013; Wernet et al., 2016). Consequently, significant changes in the supply mix of each country since 2012 are not covered. Transportation of material input and refined subparts was also accounted for.

The study addresses current technologies, both in terms of design solutions and production methods. The time horizon for the validity of data, results and conclusions is estimated to be 5–7 years based on the author's observations of development cycles in the

automotive industry. Effects of changes in the electricity production over time were not addressed explicitly, as different electricity supply was already covered by the geographical variation. Production data is expected to remain representative longer than the design data, since manufacturing of electrical traction machines is subject to less progress than product development.

The results were analyzed using life cycle impact assessment (LCIA) methods recommended by the International Reference Life Cycle Data System (ILCD) handbook (JRC-IES, 2011). This guide was developed in a European context, whereas the geographical scope of this study also includes the USA and China. Still, the aim of the ILCD handbook is to guide towards best practice of LCIA in general, and efforts to establish a global consensus on LCIA methods are ongoing but not finished (Frischknecht et al., 2016; Jolliet et al., 2014). Other LCIA methods based on national data and environmental regulation have been suggested for China (Xiaowei et al., 2010) and fully developed for the USA (Bare, 2011; US EPA, 2012). However, the "Tool for the Reduction and Assessment of Chemical and Other Environmental Impacts" (TRACI), covering the USA, use the same underlying method and data as the ILCD recommendation for several key LCIA categories such as global warming and the different aspects of toxicity (Hauschild et al., 2013; US EPA, 2012). Also, TRACI does not cover mineral resource depletion (Guinée, 2015; US EPA, 2012). For simplicity and consistency, it was decided to use the ILCD set of methods also for impacts of more regional character, e.g. eutrophication and acidification, since the European-based characterization factors can be expected to serve as reasonable proxies also for the other continents (Hauschild et al., 2013).

The damage effects of various environmental problems (e.g. climate change, respiratory health or toxicity) were investigated for two areas of protection – the natural environment and human health – using the recommended endpoint methods (aggregated LCIA results) (JRC-IES, 2011). Among the ILCD midpoint category results, i.e. the potential impact of the studied options on each environmental problem type, focus was placed on those contributing the most to the endpoint results. For resource depletion, both the endpoint (ReCiPe) (Goedkoop et al., 2013) and midpoint (CML) (Guinée et al., 2002) methods were used, since their coverage in terms of characterization factors (CFs) for REEs differs, and also since they use different approaches to evaluate the resource use, thus highlighting different aspects of resource depletion. Furthermore, a comparison was also made with newer and substantially revised CFs for the CML method (v.4.4) (Acero et al., 2017), partly due to unexpected results.

Details about the modeling of the electricity supply and transports, and the ILCD 1.0.10 compilation of LCIA methods, are provided in the SR, chapters I-K.

3. Inventory analysis

3.1. Motor design description

The data for the Nd(Dy)FeB PMSM was previously described by Nordelöf et al. (2018), and its principal design was established based on observations of existing electrical vehicle traction machines in benchmarking literature (Burress and Campbell, 2013; Burress et al., 2011; Miller, 2013; Ozpineci, 2014). Component design data for electric motors was also compiled from textbooks, scientific papers, experts, and product descriptions (Nordelöf et al., 2018). The design data was used to construct and evaluate the electromagnetically active parts of the machine, i.e. the rotor and the stator cores which produce torque during operation, in ANSYS Maxwell (ANSYS, 2015), a software tool for computational design and evaluation of electrical machine performance.

In this project, new design data was gathered for the composition of the SmCo and the Sr-ferrite magnets, and the design of the PM-assisted SynRM, to reconstruct the rotor in the original ANSYS Maxwell model (ANSYS, 2015), and enable evaluation of the two additional motor options. Fig. 1 shows the main subparts of the motors as well as how the cross sections of the rotors differ between the PMSMs, option (1) and (2), and the PM-assisted SynRM, option (3). The latter, which operates with much weaker magnets, relies to a greater extent on the reluctance principle to generate torque. In addition, when the magnet field is weaker, the motor must be longer to provide the same peak torque. Consequently, all three machines differ in their total length due to the differing strengths of the magnets, and the variation of the rotor cross sections. However, apart from the length, the stator packages have the same diameter and design in all three motors. The stators comprise distributed copper windings, as described by Nordelöf et al. (2018) for the Nd(Dy)FeB PMSM design. The ANSYS Maxwell calculations provided the amounts of electrical steel, copper and magnets in the machine core, as well as the operating efficiency in torque-speed diagrams, for each motor option.

The motors also contain several passive subparts (not contributing to the torque production), e.g. insulation materials, bearings and copper in the end-windings of the stator. Generally, these parts were modeled to represent typical design choices for automotive applications (Nordelöf et al., 2018). Especially, two passive parts contributes significantly to the total motor mass, the shaft and the housing. The shaft was modeled with a fixed diameter, but scaled with the length of each machine, as established by Nordelöf et al. (2018).

The housings of all three machine options have been modeled with identical mass, in order to set the focus on the electromagnetically active parts and to limit the influence of engineering assumptions required, because housing design offers large variability (Nordelöf et al., 2018). In the designs, this is manifested in thinner housing bodies for the longer motor options, i.e. less bulk material around the cooling channels. This modeling choice was a compromise between two alternative approaches to establishing the housing weight: either with a housing cross section size and design shifting with the maximum power value (used in the referenced LCI model), since there is a correlation between power capability and cooling requirements; or else based on the length of the motor with a fixed housing cross section size and design. The first approach would give option (3) the lowest housing mass and option (1) the highest, whereas the second approach would give option (3) the highest housing mass and option (1) the lowest. Overall, the differences in length between the motors are relatively small.

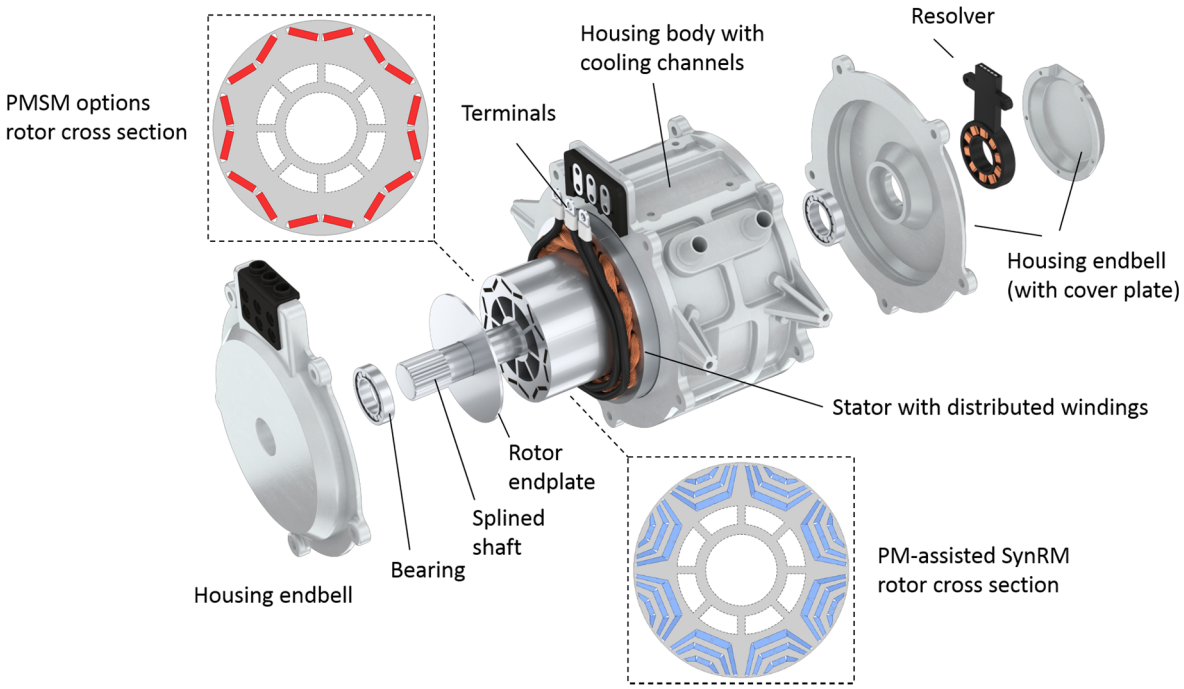

Fig. 1. Exploded sketch of the principal design common for all three electric motor options, including how the rotor laminates differ in their cross sections, with the layout of the PMSM options – the Nd(Dy)FeB PMSM (1) and the SmCo PMSM (2) – in the upper left square, and the Sr-ferrite PM-assisted SynRM (3) in the lower right square.

Table 1
Summary of the main electrical, geometrical and mass parameters for the included motor options.

Motor option	(1) Nd(Dy)FeB PMSM	(2) SmCo PMSM	(3) Sr-ferrite PM-assisted SynRM
Electric machine parameters			
Maximum power (@ 4000 rpm)	100 kW	97 kW	95 kW
Maximum torque	239 Nm		
Maximum RMS current	260 A		
Maximum current density	20 A/mm^2		
Nominal DC system voltage	400 V		
Maximum DC voltage	430 V		
Outer stator diameter	200 mm		
Active core length	127 mm	133 mm	136 mm
Magnet mass	1.26 kg	1.45 kg	1.98 kg
Total mass	44.9 kg	46.1 kg	45.6 kg

Table 1 provides a summary of the main electrical, geometrical and mass parameters for the three motor options. The Nd(Dy)FeB PMSM is the lightest of all motors and the magnets constitute 2.8% of its total mass. The design calculations showed that peak efficiencies go above 97% (SR, Fig. S3), but also that the total operating area with high efficiencies is smaller than that of the PM-assisted SynRM. The SmCo PMSM is the heaviest of the motors (with 3.1% magnets in the overall composition). The efficiency map (SR, Fig. S6) is largely similar to that of the Nd(Dy)FeB PMSM, but the highest efficiencies occur at a lower torque. Of the three machines, the PM-assisted SynRM carries the largest amount of magnets (4.1% of the total weight). The efficiency also reach above 97%. But more importantly, the operating area with efficiencies above 96% is clearly larger than for the other two options (SR, Fig. S9).

More specific details about the designs of the motor options, for example mass composition diagrams, the efficiency maps and magnet data, are reported in the underlying LCI model report (Nordelöf et al., 2017) and in the SR (chapters C, D, E and G).

3.2. Manufacturing

Large amount of electrical machine production data was collected from industry in the form of factory site visits, literature, expert interviews, machine specifications, and instruction films, for the LCI model project. Analogous with the design, this data was described by Nordelöf and Tillman (2018), including an updated dataset for the Nd(Dy)FeB magnet production chain. The inventory

data describes a complete motor factory as well as the making of electrical steel, based on investigations of Swedish facilities (Nordelöf and Tillman, 2018). Upstream raw material inputs contain both primary and secondary resources, corresponding to global market statistics as implemented in Ecoinvent 3 (Weidema et al., 2013; Wernet et al., 2016).

New data collection was carried out within this study for the SmCo and Sr-ferrite magnets. The modeling of the motor factory was adapted to shift from PMSM to PM-assisted SynRM manufacturing. Also, data was compiled for the production of rare-earth oxides (REOs) for the Nd(Dy)FeB and SmCo magnets, building on an existing dataset in Ecoinvent 3 (Weidema et al., 2013; Wernet et al., 2016), but updated and reworked with more recent energy use data and a new economic allocation procedure, based on REE price data from 2014 to 2016 (Argus, 2014; MineralPrices.com, 2016), see Section B.2 of the SR (especially Table S4) for more details.

Some manufacturing steps produce by-products in the form of scrap. In terms of mass, the vast majority is electrical steel scrap from punching stator and rotor core laminates, 24–28 kg/motor overall, when both laminates are punched in one stroke from the same sheet (Nordelöf and Tillman, 2018). Aluminum, copper and magnet scrap is also generated. Typically, scrap is collected and sold for use in new material production, but for other applications and with different quality requirements compared to newly made materials. Still, in LCA, by-products are deemed to carry a share of the environmental load of upstream processes. In this study, this issue was addressed by means of economic allocation based on the price ratio between scrap and newly made material, and some of the load relating to the original material production was allocated to the scrap (Dorrell et al., 2010; Fyhr et al., 2014; Goonan, 2016; MEPS, 2017; SteelBenchmarkerTM, 2017; USGS, 2017; Xiarchos, 2005).

Different manufacturing steps and the allocation of production scrap are explained further in the SR, in chapters B–F. Detailed schematics of the manufacturing life cycle stage for each of the three motor options are provided in Figs. S5, S8 and S11.

3.3. Use phase

The energy used during the lifetime operation of each motor option was established by applying the efficiency maps into calculations for a well-defined drive cycle. Vehicle and powertrain parameters were selected to represent a conceptualized medium-sized battery electric vehicle (similar to the Nissan Leaf and the Volkswagen e-Golf) (Grunditz and Thiringer, 2016). The WLTC drive cycle was used since it has been developed to have global representability by using statistical data for vehicles in several countries, including Sweden and the USA (Tutuianu et al., 2015). Most importantly, not all energy needed for propulsion of the vehicle was included for the use phase. Instead, to ensure a relevant comparison with the manufacturing life cycle phase, only the energy required to overcome losses caused by the electric motors (including that required to carry its own mass in terms of rolling resistance) was included. However, due to system effects, these losses not only occur in the motor itself, but also in the other powertrain components. For example, if one motor option requires a higher power input to produce the same torque, this will cause additional losses in the inverter as well. For simplification purposes, all other powertrain and vehicle parameters were set to fixed values, including the efficiencies of the other components and the charging procedure. Results for the use phase are shown in Fig. 2, per km as well as over the total driven distance of 200,000 km, both for the net energy delivered from the battery (grey) and when charging losses are included (grey and black).

A sensitivity analysis was conducted for the use phase calculations, by varying all fixed parameters within a range of typical data variation (Grunditz and Thiringer, 2016), and by applying six additional drive cycles (with different driving patterns than the WLTC). This analysis found that the use phase results are clearly stable. In particular, the PM-assisted SynRM showed the largest fluctuations in energy consumption, but the ranking order of the options remained consistent throughout all but one drive cycle with a unique low speed driving pattern.

Complete details about the use phase evaluation, including theory, drive cycles, calculation procedures, assumptions and the robustness assessment is available in chapter H of the SR.

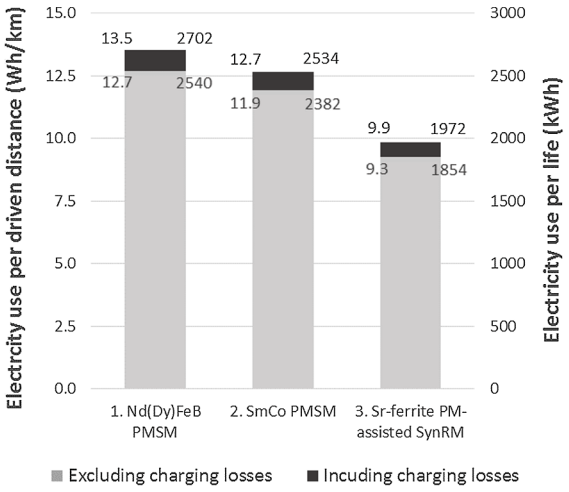

Fig. 2. Use phase energy consumption for the three motor options, per km (left axle) and for the complete use phase (right axle).

Table 2
Midpoint category results per kilometer with contributions per life cycle stage for the impact categories with largest potential to damage the natural environment and human health, and two different methods to indicate resource depletion, all recommended by the ILCD handbook (GreenDelta, 2017; JRC-IES, 2013). The resource depletion categories include the CML midpoint method (Guinée et al., 2002) presented for two different sets of CFs, and the ReCiPe endpoint method (Goedkoop et al., 2013). Acronyms used in indicator names (in addition to SI units and element abbreviations): CTU_h, comparative toxic unit for humans; SOC, soil organic carbon; PM, particulate matter.

Impact assessment category		Climate change	Human toxicity, carcinogenics	Human toxicity, non-carcinogenics	Land use	Respiratory inorganics	Resource depletion CML method, midpoint ILCD recommended CFs	Resource depletion CML method, midpoint CML v.4.4 CFs	Resource depletion ReCiPe method, endpoint ILCD v1.11 CFs
Motor option	Life cycle stage	g CO_2 eq./km	CTU_h/km	CTU_h/km	g SOC/km	g PM2.5/km	g Sb eq./km	g Sb eq./km	dollar/km
1.a:	Magnet prod.	3.21E-01	1.56E−11	1.20E−10	3.67E−01	3.25E−04	2.39E−05	1.59E−06	1.68E−05
Nd(Dy)FeB	Motor prod.	1.45E + 00	3.26E−10	4.35E−09	2.84E+00	1.93E−03	1.63E−03	8.99E−05	1.43E−04
PMSM, Sweden	Use phase	8.13E−01	1.24E−10	1.07E−09	6.57E+00	8.46E−04	1.10E−04	8.22E−06	4.70E−05
	Total	2.58E+00	4.66E−10	5.54E−09	9.78E+00	3.10E−03	1.77E−03	9.97E−05	2.07E−04
1.b:	Magnet prod.	3.22E−01	1.57E−11	1.20E−10	3.70E−01	3.25E−04	2.40E−05	1.59E−06	1.69E−05
Nd(Dy)FeB	Motor prod.	1.70E+00	3.48E−10	4.41E−09	2.80E+00	2.24E−03	1.63E−03	8.99E−05	1.55E−04
PMSM, USA	Use phase	9.36E+00	8.52E−10	3.17E−09	4.99E+00	1.13E−02	9.16E−05	7.94E−06	4.27E−04
	Total	1.14E+01	1.22E−09	7.70E−09	8.16E+00	1.39E−02	1.75E−03	9.94E−05	5.99E−04
2.a:	Magnet prod.	1.77E−01	1.11E−11	1.12E−10	3.30E−01	2.05E−04	1.54E−04	1.42E−06	9.00E−06
SmCo PMSM,	Motor prod.	1.49E+00	3.33E−10	4.44E−09	2.90E+00	1.98E−03	1.64E−03	9.10E−05	1.47E−04
Sweden	Use phase	7.62E−01	1.17E−10	1.01E−09	6.16E+00	7.94E−04	1.03E−04	7.71E−06	4.41E−05
	Total	2.43E+00	4.60E−10	5.56E−09	9.39E+00	2.98E−03	1.90E−03	1.00E−04	2.00E−04
2.b:	Magnet prod.	1.78E−01	1.12E−11	1.13E−10	3.33E−01	2.05E−04	1.54E−04	1.42E−06	9.05E−06
SmCo PMSM, USA	Motor prod.	1.74E+00	3.54E−10	4.51E−09	2.86E+00	2.29E−03	1.64E−03	9.10E−05	1.58E−04
	Use phase	8.78E+00	7.99E−10	2.97E−09	4.68E+00	1.06E−02	8.59E−05	7.45E−06	4.00E−04
	Total	1.07E+01	1.17E−09	7.59E−09	7.87E+00	1.31E−02	1.88E−03	9.99E−05	5.68E−04
3.a:	Magnet prod.	1.52E−01	5.26E−12	2.00E−11	1.08E−01	1.80E−04	1.87E−04	6.31E−08	6.30E−06
Sr-ferrite PM-assisted SynRM,	Motor prod.	1.50E+00	3.28E−10	4.49E−09	2.93E+00	2.00E−03	1.64E−03	9.16E−05	1.48E−04
Sweden	Use phase	5.93E−01	9.07E−11	7.82E−10	4.79E+00	6.18E−04	8.04E−05	6.00E−06	3.43E−05
	Total	2.25E+00	4.24E−10	5.29E−09	7.83E+00	2.79E−03	1.91E−03	9.76E−05	1.89E−04
3.b:	Magnet prod.	1.53E−01	5.45E−12	2.03E−11	1.13E−01	1.80E−04	1.87E−04	6.60E−08	6.37E−06
Sr-ferrite PM-assisted SynRM,	Motor prod.	1.77E+00	3.50E−10	4.55E−09	2.88E+00	2.32E−03	1.64E−03	9.16E−05	1.60E−04
USA	Use phase	6.83E+00	6.22E−10	2.31E−09	3.64E+00	8.25E−03	6.69E−05	5.80E−06	3.12E−04
	Total	8.76E+00	9.78E−10	6.89E−09	6.64E+00	1.07E−02	1.90E−03	9.74E−05	4.78E−04

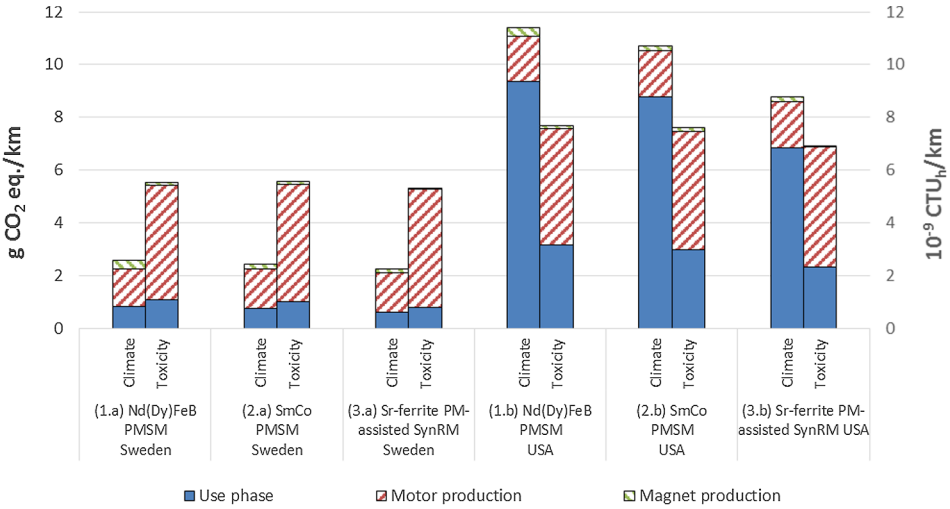

Fig. 3. Results for climate change (units to the left) and non-carcinogenic human toxicity (units to the right) impact categories, stated per kilometer. Contributions per life cycle stage.

4. Results and discussion

4.1. Impacts on the natural environment and human health

Climate change and land use were found to be the essential contributors among the types of impact that have potential effects on the natural environment for all motor options, according to the endpoint results for the ecosystems category in the method recommended by the ILCD handbook (JRC-IES, 2013). Similarly, the investigation of midpoint category contributions to the damage on human health, demonstrated that there is a risk especially due to toxicity, but also on account of respiratory inorganics and climate change. In contrast, it was found that acidification, eutrophication, ozone depletion, photochemical smog and radioactive radiation are less relevant, with negligible contributions to potential endpoint effects.

Accordingly, the most important midpoint categories for impacts on the natural environment and human health were investigated using the ILCD midpoint category recommendations: climate change, human toxicity for carcinogens and non-carcinogens, land use and respiratory inorganics. The results are compiled in Table 2. The two categories assessed to be the most important overall, i.e. climate change and toxicity, are also illustrated graphically in Fig. 3.

All results (both Table 2 and Fig. 3) are reported for three stages: magnet production, motor production and the use phase. Magnet production represents the making of magnets in China and the transportation to Sweden or the USA, respectively. Motor production refers to the manufacturing of all other subcomponents and the assembly, and the use phase represents the electricity production required to compensate for the losses caused by each motor type during operation, due to its mass and efficiency.

For climate change, there is a large difference between the studied geographical locations, i.e. production and operation in Sweden (a) versus in the USA (b), coupled to the carbon intensity of the electricity supply mixes. In the US context, where the electricity supply is more carbon intensive, efficient use of energy during operation is the main determining factor between the motor types, with the PM-assisted SynRM as the least polluting alternative. The magnet production has a similar pattern among the options as the use phase, but with a minor contribution overall. The motor production stage is reversed in ranking order, but comparable in size for all options. In the Swedish context, motor production is the dominant phase with regard to CO_2-emissions. Upstream steel manufacture is the largest contributor, followed by the production of aluminum for the housing and copper for the windings. In total, manufacturing accounts for 1.8–2.0 CO_2-eq./km for the Nd(Dy)FeB PMSM (1) and 1.7–1.9 CO_2-eq./km for the other two options (2 and 3), as can be seen in Table 2. The use phase carbon emissions are caused by the charging required to compensate for losses generated in and by the electric motors. For reference, it can be noted that the additional lifetime charging demand to propel the complete vehicle (covering for the propulsion work and other powertrain losses) on the WLTC, was calculated to produce 6.7 g CO_2 eq./km in Sweden and 77 g in the USA.

Contrary to climate change, the land use is larger in Sweden than the USA (Table 2). Again, the total results are ultimately dependent on the use phase energy consumption, making the PM-assisted SynRM the most preferable option, with the SmCo PMSM as the second best. The main load is occupation of land for intensive forestry, which can be explained by the relatively large share of biomass in Swedish power production. In the US, the major factor is transformation of natural land to mineral and fossil extraction sites, also driven by power production.

Two different human toxicity categories were assessed: for carcinogens and for non-carcinogens (Table 2). The latter category is displayed in Fig. 3. Overall, the two categories show similar patterns, with the PM-assisted SynRM as the best and the Nd(Dy)FeB PMSM as the worst alternative, coupled to the variability in motor efficiency and the related impact of the use phase. The relative shares of production and use phase differ between the toxicity categories. However, within each category, the motor production

contribution is very similar in absolute numbers for all options.

Copper production gives important contributions in both toxicity categories, for all motor options. In the non-carcinogenic impact category it is the dominant contributor throughout all alternatives, counting all life cycle stages. Long term emissions of heavy metals to ground water, deriving from sulfidic tailings of the mining operation, constitute a main problem. Leakage of arsenic, zinc and copper causes non-carcinogenic impact. Carcinogenic chromium is also emitted from copper production, as well as from other extraction of raw materials and fossil fuels.

The burden on human health is further increased by emissions of respiratory inorganics, i.e. particles, mainly during the motor use. These results largely co-vary with the climate change category (Table 2), since they are mainly caused by airborne emissions from electricity production related to combustion, most obviously for the motors operated in the USA. In contrast to climate change, copper production is the largest emitting activity of the production stage, with sulfur dioxide being the key emission.

The complete LCIA results (including the impact categories found less relevant) are illustrated with figures and have additional comments in chapter K of the SR.

4.2. Resource depletion

The results for depletion of resources shown in Table 2 are more ambiguous than those for ecosystems and human health. More specifically, the results for the midpoint resource depletion indicator (CML method) initially gave surprising results when the CFs endorsed by the ILCD handbook (ILCD 1.0.10 package for open LCA) (GreenDelta, 2017; JRC-IES, 2013) were used. An unfortunate combination of exceptionally high CFs for typical trace metals, i.e. indium and cadmium, and a probable overestimation of the same metals in upstream infrastructure datasets of Ecoinvent, for example in waste treatment facilities and melting furnaces for aluminum, brought about a confounding dominance of these metals in the results for resource depletion (76–84% of the values stated for the motor production stage in Table 2, considering all options), although they are not constituents of any of the investigated motors. In fact, indium was found to dominate the resource depletion results for global aluminum alloy production, despite it being modeled with about 80% recycled scrap (Weidema et al., 2013; Wernet et al., 2016), and given the fact that indium can rarely be found at all in bauxite (Briskey, 2005; Dentoni et al., 2014).

As a response, the impact on resource depletion was assessed using three different approaches in parallel: (1) using the CML method (Guinée et al., 2002) with ILCD's recommended CFs (GreenDelta, 2017; JRC-IES, 2013), but with an additional analysis excluding indium and cadmium; (2) using CML v.4.4 (Hauschild et al., 2013), with updated CFs (including a reduction of the CFs for indium and strontium with more than 80,000 and 250,000, respectively – other example values are reported in Table S39 of the SR); and (3) using the endpoint indicator from ReCiPe (Goedkoop et al., 2013), also endorsed by the ILCD handbook (Hauschild et al., 2013). In the results for approach (1) the contribution of the motor production stage decreased from about 1.6 mg Sb eq./km (see Table 2) to about 0.2 mg Sb eq./km for all options, when indium and cadmium was disregarded. With the use phase contribution unchanged and roughly the same for all options (1.a–3.b), the clear difference in the load of the magnets became the deciding factor for the ranking among the options, with the PM-assisted SynRM as the worst alternative and the SmCo PMSM as the second worst. Key issues are the depletion of strontium for the Sr-ferrite magnets and cobalt for the SmCo magnets.

In this assessment, approach (1), REEs were included but were found to be less significant. It is notable that REEs which are relatively abundant in the Earth's crust compared to other metals, but which are found mixed and in low concentrations (Gupta and Krishnamurthy, 2005; Wübbeke, 2013), are not indicated as problematic by this LCIA method. The CML midpoint method emphasizes the long term scarcity of elements on Earth based on estimates of ultimate reserves and extraction rates (Guinée et al., 2002). This method is sensitive to shifts in these estimates, made for different sets of CFs.

Accordingly, the results for approach (2) with CML v.4.4 CFs are very different (Table 2). Overall, they indicate a much lower level of depletion as a whole, with no clear difference among the options, and a total dominance of the motor production stage. This was expected since CML v.4.4 has a separate indicator for mineral depletion, without fossil fuels (Hauschild et al., 2013).

Both assessments at midpoint showed that depletion coupled to motor production is largely caused by copper use, including other metals occurring in the same ore, such as silver and lead. REEs have no CFs in CML v.4.4 (Hauschild et al., 2013).

In contrast, the ReCiPe endpoint method, approach (3), focuses on existing mineral deposits with a shorter time horizon (Goedkoop et al., 2013; Hauschild et al., 2013). Other results can therefore be expected from this resource depletion assessment. Overall, a larger emphasis is placed on the depletion of fossil fuels, which results in a similar pattern and the same ranking order among the options as for the midpoint climate change results (Table 2). However, for the production of the motor and magnets, the results confirm copper production as a key activity for resource depletion. Among the magnets, the Nd(Dy)FeB type has the highest load, despite the fact that CFs are lacking for REEs in this method. Instead, the impact of Nd(Dy)FeB magnets is due to raw material extraction for the Chinese electricity supply. If REEs had been included, they would have added load on the PMSM options and most likely reinforced current results, since there are few existing large REO deposits viable for long term operation, and they are being heavily explored.

Indeed, the relevance and applicability of the currently available LCIA methods covering depletion of natural resources, and mineral resource assessment in particular, is being debated in LCA methodology literature. For a more thorough discussion, please read Drielsma et al. (2016); Hauschild et al. (2013) or Sonderegger et al. (2017). More details are presented in sections K.1.2 and K.2.7 of the SR about the CFs available for the different methods, and versions of methods, included in the study for assessing resource depletion.

4.3. Robustness of results

A sensitivity analysis of key parameters was conducted to test the stability of the LCIA results. All midpoint categories identified as important for the potential damage on the natural environmental and human health, and all applied resource categories were tested. High and low values (+25% and −20% for the PMSM options, and +32% and −29% for the PM-assisted SynRM) for the use phase energy consumption of the three motor types were included, based on the results of the previous use phase sensitivity analysis. The allocation factor for steel scrap was varied up to 100% and down to 0%. The aluminum housing mass (± 20%) and total lifetime driven distance (± 25%) were also varied. The results were found to be very robust and without any major shifts in ranking order for any category in comparison with original results; only in two instances two options with adjacent ranking swapped order, for all variation of key parameters. The PM-assisted SynRM remained the consistently best option for all parameter settings and throughout all categories, except for the CML midpoint resource depletion results with the CFs endorsed by the ILCD handbook, as was the case in the original results.

The robustness assessment is presented in detail in Table S40 of the SR.

4.4. Concluding implications for motor design and material recovery

Overall, the PM-assisted SynRM has the least environmental burden of the three motor options due to its broad working area with high efficiency compared to the PMSM motor options. Regardless of the background system, high efficiency decreases the impact of the use phase and thereby also significantly impacts on climate change, land use, human toxicity and respiratory health. This finding is in line with previous studies (Hernandez et al., 2017b).

However, electric motor design includes tradeoffs between many parameters. Striving for increased efficiency without any additional guidance can lead to larger machines, whereby load is shifted to the production phase, which may partly neutralize the use phase benefits. The results show that both copper and aluminum use should preferably be reduced, for example by minimizing end-windings and by keeping the housing as slim as possible. The climate impact of electrical steel can be addressed by selecting methods for manufacturing based on punching in segments which generate less scrap compared to punching laminates in one piece, both for the stator and the rotor. Direct recycling routes for electrical steel scrap back to the supplier would also decrease the load of the steel, compared to current recycling procedures for production scrap.

Magnets were not found to be a key contributor of emissions. The impact of magnets is mainly indirect, i.e. their properties influence the amount of other materials used in the design. Still, the results for resource depletion were found to be uncertain and divergent between the different evaluation methods.

Moreover, recycling of the entire motor at its end-of-life is an obvious approach to further reducing the load of all machine options, albeit that it was not quantified in this study. Hernandez et al. (2017a) find that recycling processes give a very positive effect on their overall results when they model recycling as a closed loop. However, such material recovery back to original quality is very unlikely in today's shredder-based recycling processes for the end-of-life of vehicles (Söderman and Ingemarsdotter, 2014; Tasala Gradin et al., 2013). The fact that magnets in electric motors are not being recycled at all (Andersson et al., 2016; Binnemans et al., 2013; Tasala Gradin et al., 2013), while other metals are, implies that any modeling of current recycling practices would lead to an increased share of impact from magnet production in LCAs of electric motors. Still, given that EoL processing requires additional energy use and that the study already accounts for inputs of secondary raw materials, it is not expected that an inclusion of EoL by shredding in the study would cause any significant shift in the results. But, without a more thorough investigation of feasible EoL routes, it would add additional modeling uncertainty for all options, and therefore it was left out since the primary audience of the study consists of actors that develop and manufacture electric traction motors.

Furthermore, a high degree of quality recovery of copper from vehicle traction machines cannot be expected in the current recycling system (Brahmst, 2006; Söderman and Ingemarsdotter, 2014; Tasala Gradin et al., 2013). Therefore, in order to enable a real reduction of the load on human health and resource use caused by copper production, material recycling must be improved beyond current practices. This could be accomplished by disassembling motors from the vehicle prior to shredding and by designing to allow further easy dismantling into pure material fractions suitable for recycling.

Future work relating to this study will focus on thorough investigations and scenario building of possible future dismantling, remanufacturing, reuse and recycling pathways, in order to provide a solid foundation for further analysis of the EoL stage.

Acknowledgement

The authors would like to express their gratitude to the Swedish Energy Agency and the Area of Advance Energy at Chalmers University of Technology for financing the project.

Appendix A. Supplementary material

A supplementary information report accompanies this article, with detailed data descriptions, and additional figures and tables. It can be found online at https://doi.org/10.1016/j.trd.2018.11.004.

References

ABB, 2002. Environmental Product Declaration: AC Low Voltage Cast Iron Motor, Type M3BP 315, Release/Version May 2002. ABB Oy/BA Electrical Machines, LV Motors, Vaasa, Finland (Document code: LV Motors/EPD M3BP315 GB 05-2002 3GZF500931-22).

Acero, A.P., Rodríguez, C., Ciroth, A., 2017. LCIA methods: Impact assessment methods in Life Cycle Assessment and their impact categories. GreenDelta GmbH, Berlin, Germany (13 February 2017, Version 1.5.6).

Andersson, M., Ljunggren Söderman, M., Sandén, B.A., 2016. Are scarce metals in cars functionally recycled? Waste Manage. https://doi.org/10.1016/j.wasman.2016.06.031.

ANSYS, 2015. ANSYS® Electromagnetic Suite, Maxwell 2015.1.0, 16.1.0 ed. ANSYS, Inc. (ISBN/ISSN, Electrical machine design and evaluation software).

Argus, 2014. Rare Earths: Rare Earth Market Prices, News and Analysis. Argus Media Ltd, London, UK (Release/version 2 October 2014).

Bare, J., 2011. TRACI 2.0: the tool for the reduction and assessment of chemical and other environmental impacts 2.0. Clean Technol. Environ. Policy 13, 687–696. https://doi.org/10.1007/s10098-010-0338-9.

Binnemans, K., Jones, P.T., Blanpain, B., Van Gerven, T., Yang, Y., Walton, A., Buchert, M., 2013. Recycling of rare earths: a critical review. J. Clean. Prod. 51, 1–22. https://doi.org/10.1016/j.jclepro.2012.12.037.

Brahmst, E., 2006. Copper in End-of-Life Vehicle Recycling. Manufacturing, Engineering & Technology Group, Center for Automotive Research, Ann Arbor, Michigan, USA (November 2006, Prepared for the Copper Development Association).

Briskey, J.A., 2005. Indium in Lead-Zinc and Other Mineral Deposits — A Reconnaissance Survey of 1118 Indium Analyses Published Before 1985. U.S. Geological Survey, U.S. Department of the Interior, Reston, Virginia, USA (Open-File Report 2005-1209).

Burress, T., Campbell, S., 2013. Benchmarking EV and HEV power electronics and electric machines. In: Transportation Electrification Conference and Expo (ITEC), 2013 IEEE 16–19 June 2013. IEEE, Detroit, MI, USA, pp. 1–6.

Burress, T.A., Campbell, S.L., Coomer, C.L., Ayers, C.W., Wereszczak, A.A., Cunningham, J.P., Marlino, L.D., Seiber, L.E., Lin, H.T., 2011. Evaluation of the 2010 Toyota prius hybrid synergy drive system. Electrical and Electronics Systems Research Division, Oak Ridge National Laboratory, US Department of Energy, USA (March 2011, ISBN/ISSN ORNL/TM-2010/253).

Chan, C.C., 2007. The state of the art of electric, hybrid, and fuel cell vehicles. Proc. IEEE 95, 704–718. https://doi.org/10.1109/JPROC.2007.892489.

Cullbrand, K., Fråne, A., Jensen, C., 2015. Utökad demontering av personbilar – Utvärdering av demontering- och fragmenteringsförsök av 220 personbilar. IVL Svenska Miljöinstitutet AB, Stockholm, Sweden (Report no C142. Swedish EoL study of how increased disassembly before shredding can influence material recycling for passenger vehicles).

Dentoni, V., Grosso, B., Massacci, G., 2014. Environmental Sustainability of the Alumina Industry in Western Europe. Sustainability 6, 9477.

Dorrell, D.G., Knight, A.M., Popescu, M., Evans, L., Staton, D.A., 2010. Comparison of different motor design drives for hybrid electric vehicles. In: IEEE Energy Conversion Congress and Exposition, 12–16 Sept. 2010, pp. 3352–3359.

Drielsma, J.A., Russell-Vaccari, A.J., Drnek, T., Brady, T., Weihed, P., Mistry, M., Simbor, L.P., 2016. Mineral resources in life cycle impact assessment—defining the path forward. Int. J. Life Cycle Assess. 21, 85–105. https://doi.org/10.1007/s11367-015-0991-7.

Ellingsen, L.A.-W., Hung, C.R., Strømman, A.H., 2016. Lifecycle impacts of lithium-ion batteries: a review. EVS29 International Battery, Hybrid and Fuel Cell Electric Vehicle Symposium, June 19–22, 2016. Montréal, Québec, Canada.

European Commission, 2015. Closing the Loop – An EU Action Plan for the Circular Economy. European Commission, Brussels, Belgium (COM(2015) 614/2).

European Commission, 2018. Report on Critical Raw Materials and the Circular Economy. European Commission, Brussels, Belgium (SWD(2018) 36 final).

Frischknecht, R., Fantke, P., Tschümperlin, L., Niero, M., Antón, A., Bare, J., Boulay, A.-M., Cherubini, F., Hauschild, M.Z., Henderson, A., Levasseur, A., McKone, T.E., Michelsen, O.i., Canals, L.M., Pfister, S., Ridoutt, B., Rosenbaum, R.K., Verones, F., Vigon, B., Jolliet, O., 2016. Global guidance on environmental life cycle impact assessment indicators: progress and case study. Int. J. Life Cycle Assess. 21, 429–442. https://doi.org/10.1007/s11367-015-1025-1.

Fyhr, P., Ståhl, J.E., Andersson, M., 2014. Statistical interfaces for production of a permanent magnet based rotor. In: 4th International Electric Drives Production Conference (EDPC), Sept. 30, 2014–Oct. 1, 2014, pp. 1–6.

Goedkoop, M.J., Heijungs, R., Huijbregts, M., De Schryver, A., Struijs, J., Van Zelm, R., 2013. ReCiPe 2008, A Life Cycle Impact Assessment Method Which Comprises Harmonised Category Indicators at the Midpoint and the Endpoint Level – Report I: Characterisation, first (revised) ed. Ministry of Housing, Spatial Planning and Environment (VROM), The Netherlands.

Goonan, T.G., 2016. United States Copper Metal and Scrap Use and Trade Patterns, 1995–2014. U.S. Geological Survey, U.S. Department of the Interior, Reston, Virginia, USA (Scientific Investigations Report 2016–5075).

Graedel, T.E., Harper, E.M., Nassar, N.T., Nuss, P., Reck, B.K., 2015. Criticality of metals and metalloids. Proc. Nat. Acad. Sci. 112, 4257–4262. https://doi.org/10.1073/pnas.1500415112.

GreenDelta, 2017. LCIA Methods: ILCD 2011 v1.0.10 Method Update in openLCA. GreenDelta GmbH, Berlin, Germany Version 1.1, ILCD 2011 [v1.0.10, August 2016].

Grunditz, E.A., Thiringer, T., 2016. Performance analysis of current BEVs – based on a comprehensive review of specifications. IEEE Trans. Transp. Electr. https://doi.org/10.1109/TTE.2016.2571783.

Guinée, J.B., 2015. Selection of impact categories and classification of LCI results to impact categories. In: Hauschild, M.Z., Huijbregts, M.A.J. (Eds.), Life Cycle Impact Assessment. Springer, Dordrecht (ISBN/ISSN).

Guinée, J.B., Gorrée, M., Heijungs, R., Huppes, G., Kleijn, R., Koning, A.d., Oers, L.v., Wegener Sleeswijk, A., Suh, S., Udo de Haes, H.A., Bruijn, H.D., Duin, R.v., Huijbregts, M.A.J., 2002. Handbook on life cycle assessment. Operational guide to the ISO standards. I: LCA in perspective. IIa: Guide. IIb: Operational annex. III: Scientific background. In: Guinée, J.B. (Ed.), Centrum Milieukunde Leiden (CML). Leiden University. Kluwer Academic Publishers, Dordrecht, pp. 692 (ISBN/ISSN ISBN 1-4020-0228-9).

Gupta, C.K., Krishnamurthy, N., 2005. Extractive Metallurgy of Rare Earths. CRC Press, Boca Raton, Florida.

Hauschild, M., Goedkoop, M., Guinée, J., Heijungs, R., Huijbregts, M., Jolliet, O., Margni, M., Schryver, A., Humbert, S., Laurent, A., Sala, S., Pant, R., 2013. Identifying best existing practice for characterization modeling in life cycle impact assessment. Int. J. Life Cycle Assess. 18, 683–697. https://doi.org/10.1007/s11367-012-0489-5.

Hawkins, T., Gausen, O., Strømman, A., 2012. Environmental impacts of hybrid and electric vehicles – a review. Int. J. Life Cycle Assess. 17, 997–1014. https://doi.org/10.1007/s11367-012-0440-9.

Hernandez, M., Messagie, M., De Gennaro, M., Van Mierlo, J., 2017a. Resource depletion in an electric vehicle powertrain using different LCA impact methods. Resour. Conserv. Recycl. 120, 119–130. https://doi.org/10.1016/j.resconrec.2016.11.005.

Hernandez, M., Messagie, M., Hegazy, O., Marengo, L., Winter, O., Mierlo, J., 2017b. Environmental impact of traction electric motors for electric vehicles applications. Int. J. Life Cycle Assess. 22, 54–65. https://doi.org/10.1007/s11367-015-0973-9.

Jin, H., Afiuny, P., McIntyre, T., Yih, Y., Sutherland, J.W., 2016. Comparative life cycle assessment of NdFeB magnets: virgin production versus magnet-to-magnet recycling. Procedia CIRP 48, 45–50. https://doi.org/10.1016/j.procir.2016.03.013.

Jolliet, O., Frischknecht, R., Bare, J., Boulay, A.M., Bulle, C., Fantke, P., Gheewala, S., Hauschild, M., Itsubo, N., Margni, M., McKone, T.E., 2014. Global guidance on environmental life cycle impact assessment indicators: findings of the scoping phase. Int. J. Life Cycle Assess. 19, 962–967. https://doi.org/10.1007/s11367-014-0703-8.

JRC-IES, 2011. International Reference Life Cycle Data System (ILCD) Handbook – Recommendations for Life Cycle Impact Assessment in the European Context, first ed. Publications Office of the European Union: European Commission – Joint Research Centre – Institute for Environment and Sustainability, Luxemburg (November 2011, EUR 24571 EN).

JRC-IES, 2013. Characterisation Factors of the ILCD Recommended Life Cycle Impact Assessment Methods – Database and Supporting Information, updated ed. Publications Office of the European Union: European Commission – Joint Research Centre – Institute for Environment and Sustainability, Luxemburg (Februray 20, 2013, EUR 25167 EN – 2012).

Koltun, P., Tharumarajah, A., 2014. Life cycle impact of rare earth elements. ISRN Metall. 2014, 10. https://doi.org/10.1155/2014/907536.

MEPS, 2017. MEPS – North American Stainless Steel Prices [Online]. MEPS (International) LTD, Sheffield, United Kingdom (accessed March 12, 2017).

Miller, J.M., 2013. Oak Ridge National Laboratory Annual Progress Report for the Power Electronics and Electric Motors Program, Annual Progress Report – Advanced Power Electronics and Electric Motors. US Department of Energy: Electrical and Electronics Systems Research Division, Oak Ridge National Laboratory, USA (November 2013, ORNL/TM-2013/498).

MineralPrices.com, 2016. Rare Earth Metals [Online]. MineralPrices.com, Toronto, Ontario, Canada (accessed 3 November 2016).
Nakada, T., Ishikawa, S., Oki, S., 2014. Development of an Electric Motor for a Newly Developed Electric Vehicle, SAE Technical Paper 2014-01-1879, 2014. SAE International. ISBN/ISSN. https://doi.org/10.4271/2014-01-1879.
Nordelöf, A., Grunditz, E., Tillman, A.-M., Thiringer, T., Alatalo, M., 2017. A Scalable Life Cycle Inventory of an Electrical Automotive Traction Machine – Technical and Methodological Description. Department of Energy and Environment, Divisions of Environmental Systems Analysis & Electric Power Engineering, Chalmers University of Technology, Gothenburg, Sweden (ESA report no. 2016:4 (version 1.01 updated 2017)).
Nordelöf, A., Grunditz, E., Tillman, A.-M., Thiringer, T., Alatalo, M., 2018. A scalable life cycle inventory of an electrical automotive traction machine—Part I: design and composition. Int. J. Life Cycle Assess. 23, 55–69. https://doi.org/10.1007/s11367-017-1308-9.
Nordelöf, A., Messagie, M., Tillman, A.-M., Ljunggren Söderman, M., Van Mierlo, J., 2014. Environmental impacts of hybrid, plug-in hybrid, and battery electric vehicles—what can we learn from life cycle assessment? Int. J. Life Cycle Assess. 19, 1866–1890. https://doi.org/10.1007/s11367-014-0788-0.
Nordelöf, A., Tillman, A.-M., 2018. A scalable life cycle inventory of an electrical automotive traction machine—Part II: manufacturing processes. Int. J. Life Cycle Assess. 23, 295–313. https://doi.org/10.1007/s11367-017-1309-8.
Ozpineci, B., 2014. Oak Ridge National Laboratory Annual Progress Report for the Power Electronics and Electric Motors Program, Annual Progress Report – Advanced Power Electronics and Electric Motors. US Department of Energy: Electrical and Electronics Systems Research Division, Oak Ridge National Laboratory, US [ORNL/SPR-2014/532].
Peters, J.F., Baumann, M., Zimmermann, B., Braun, J., Weil, M., 2017. The environmental impact of Li-ion batteries and the role of key parameters – a review. Renew. Sustain. Energy Rev. 67, 491–506. https://doi.org/10.1016/j.rser.2016.08.039.
Ramakrishnan, K., Stipetic, S., Gobbi, M., Mastinu, G., 2016. Multi-objective optimization of electric vehicle powertrain using scalable saturated motor model. In: Eleventh International Conference on Ecological Vehicles and Renewable Energies (EVER), 6–8 April 2016, pp. 1–6.
Sizov, G.Y., Ionel, D.M., Demerdash, N.A.O., 2011. Multi-objective optimization of PM AC machines using computationally efficient - FEA and differential evolution. In: IEEE International Electric Machines & Drives Conference (IEMDC), 15–18 May 2011, pp. 1528–1533.
Sonderegger, T., Dewulf, J., Fantke, P., de Souza, D.M., Pfister, S., Stoessel, F., Verones, F., Vieira, M., Weidema, B., Hellweg, S., 2017. Towards harmonizing natural resources as an area of protection in life cycle impact assessment. Int. J. Life Cycle Assess. 22, 1912–1927. https://doi.org/10.1007/s11367-017-1297-8.
Sprecher, B., Xiao, Y., Walton, A., Speight, J., Harris, R., Kleijn, R., Visser, G., Kramer, G.J., 2014. Life cycle inventory of the production of rare earths and the subsequent production of NdFeB rare earth permanent magnets. Environ. Sci. Technol. 48, 3951–3958. https://doi.org/10.1021/es404596q.
Sprecher, B., Xiao, Y., Walton, A., Speight, J., Harris, R., Kleijn, R., Visser, G., Kramer, G.J., 2014b. Life Cycle Inventory of the Production of Rare Earths and the Subsequent Production of NdFeB Rare Earth Permanent Magnets – Supporting Information. Institute of Environmental Sciences (CML), Leiden University, The Netherlands, pp. 13 (ISBN/ISSN. Supporting Information for Environmental Science & Technology).
SteelBenchmarker™, 2017. Price History: Tables and Charts. World Steel Dynamics Inc, New Jersey, USA (report #261, accessed from www.steelbenchmarker.com).
Söderman, M.L., Ingemarsdotter, E., 2014. Användning och återvinning av potentiellt kritiska material – Kunskapsöversikt. Division of Environmental Systems Analysis, Department of Energy and Environment, Chalmers University of Technology, Gothenburg, Sweden (Report no 2014:20).
Tasala Gradin, K., Luttropp, C., Björklund, A., 2013. Investigating improved vehicle dismantling and fragmentation technology. J. Clean. Prod. 54, 23–29. https://doi.org/10.1016/j.jclepro.2013.05.023.
Treyer, K., Bauer, C., 2016a. Life cycle inventories of electricity generation and power supply in version 3 of the ecoinvent database—part I: electricity generation. Int. J. Life Cycle Assess. 21, 1236–1254. https://doi.org/10.1007/s11367-013-0665-2NS.
Treyer, K., Bauer, C., 2016b. Life cycle inventories of electricity generation and power supply in version 3 of the ecoinvent database—part II: electricity markets. Int. J. Life Cycle Assess. 21, 1255–1268. https://doi.org/10.1007/s11367-013-0694-x.
Tutuianu, M., Bonnel, P., Ciuffo, B., Haniu, T., Ichikawa, N., Marotta, A., Pavlovic, J., Steven, H., 2015. Development of the World-wide harmonized Light duty Test Cycle (WLTC) and a possible pathway for its introduction in the European legislation. Transport. Res. Part D: Transport Environ. 40, 61–75. https://doi.org/10.1016/j.trd.2015.07.011.
US EPA, 2012. Tool for the Reduction and Assessment of Chemical and Other Environmental Impacts (TRACI) TRACI version 2.1 – User's Guide. Sustainable Technology Division, National Risk Management Research Laboratory, Office of Research and Development, U.S. Environmental Protection Agency, Cincinnati, Ohio, USA (July 2012, EPA/600/R-12/554).
USGS, 2017. Mineral Industry Surveys: Aluminum in December 2016. U.S. Geological Survey, U.S. Department of the Interior, Reston, Virginia, USA (February 2017).
Walton, A., Yi, H., Rowson, N.A., Speight, J.D., Mann, V.S.J., Sheridan, R.S., Bradshaw, A., Harris, I.R., Williams, A.J., 2015. The use of hydrogen to separate and recycle neodymium–iron–boron-type magnets from electronic waste. J. Clean. Prod. 104, 236–241. https://doi.org/10.1016/j.jclepro.2015.05.033.
Weidema, B.P., Bauer, C., Hischier, R., Mutel, C., Nemecek, T., Reinhard, J., Vadenbo, C.O., Wernet, G., 2013. The Ecoinvent Database: Overview and Methodology, Data Quality Guideline for the Ecoinvent Database Version 3 [Online]. The Centre for Life Cycle Inventories, Switzerland.
Wernet, G., Bauer, C., Steubing, B., Reinhard, J., Moreno-Ruiz, E., Weidema, B., 2016. The ecoinvent database version 3 (part I): overview and methodology. Int. J. Life Cycle Assess. 21, 1218–1230. https://doi.org/10.1007/s11367-016-1087-8.
Wübbeke, J., 2013. Rare earth elements in China: policies and narratives of reinventing an industry. Resour. Policy 38, 384–394. https://doi.org/10.1016/j.resourpol.2013.05.005.
Xiaowei, W., Fangyi, L., Jianfeng, L., Liming, W., 2010. A life cycle impact assessment method based on multi-environmental dimension. In: 5th International Conference on Responsive Manufacturing – Green Manufacturing (ICRM 2010), 11–13 Jan. 2010, pp. 206–214.
Xiarchos, I.M., 2005. Steel: Price Links between Primary and Scrap Markets, Southern Agricultural Economics Association Annual Meetings, February 5–9, 2005. West Virginia University, Little Rock, Arkansas, Morgantown, West Virginia.
Zakotnik, M., Tudor, C.O., 2015. Commercial-scale recycling of NdFeB-type magnets with grain boundary modification yields products with 'designer properties' that exceed those of starting materials. Waste Manag. 44, 48–54. https://doi.org/10.1016/j.wasman.2015.07.041.

Glossary/list of abbreviations

CF: characterization factor
CML: acronym name, originally Centrum voor Milieukunde Leiden
ILCD: name, International Reference Life Cycle Data System
LCA,: life cycle assessment
LCI,: life cycle inventory
LCIA,: life cycle impact assessment;
Nd(Dy)FeB: neodymium-dysprosium-iron-boron
PM-assisted SynRM: permanent magnet-assisted synchronous reluctance machine
PMSM: permanent magnet synchronous machine
ReCiPe: acronym name
REE,: rare-earth element
REO: rare-earth oxide
Rpm: rotations per minute
SmCo: samarium-cobalt
Sr-ferrite: strontium-ferrite
WLTC: the worldwide harmonized light duty driving test cycle